BOLETIN DE LA SOCIEDAD ESPAÑOLA DE
Cerámica y Vidrio
A R T I C U L O

Densification and crystalization kinetics of mullite diphasic gels from non_isothermal dilatometry experiments

F. ORGAZ

Instituto de Cerámica y Vidrio, CSIC.
Departamento de Electro Cerámica , 28049 Madrid.

Mullite (3 AI2O3_2 SiO2) was processed by mixing silica and alumina colloids at pH below 3 in a high shear blender. The gels were sieved to ‹ 125 microns and cold isostatically pressed to form rods. The various processes involved during the sintering process such as condensation-polymerization and the competition between mullite crystallization and densification were analysed from constant heating rate equations and rate controlled sintering dilatometer experiments. Changes in the slopes permitted the identification of such processes and the activation energy for mullitization was calculated. Fast firing (20-30 K/min) in the critical mullitization temperature range of 1230-1505"C and low heating rates (2-3 K/min) in the viscous flow densification intervals of below 1230ºC and higher than 1505 gives rise to near full density and fine grain microstructures of sintered mullite. Fast firing and high (0.5 to 1 % /min) densification rate controlled processes seem to be the most suitable approaches to high density gel processed mullite. Amorphous silica is the rate controlling mechanism for the viscous flow densification process before alumina is solved and nucleation and crystallization of mullite appears. Deviations from the linear Frenkel model for viscous flow are also observed.

Keywords: mullite, colloidal, sol-gel, kinetics, dilatometry.

Cinética de cristalización y sinterización de geles difásicos de mullita a partir experimentos no isotérmicos de dilatometría

Mullita de composición 3 Al2O3 -2 SiO2 ha sido preparada mezclando coloides de sílice y alúmina en un mezclador de alta velocidad a pH<3. Los geles formados eran secados, tamizados por debajo de 125 micras y prensados isostáticamrente para formar varillas de unos 6 mm de diámetro. Los diferentes procesos que ocurren durante el proceso de sinterización, tales como polimerización- condensación y la competición entre cristalización y densificación, han sido analizados utilizando las ecuaciones de ecuaciones de velocidad de calentamiento constantte y experimentos de dilatometría utilizando un software que permite realizar ensayos a velocidad de contracción constante. Cambios en las pendientes han permitido la identificación de tales procesos y el calculo de la energia de activación para la formación de mullita. Calentamiento rápido (20-30 K/min) en el rango critico de formación de mullita entre 1230-1505ºC y bajas velocidades de calentamiento (2-3 K/min) en las zonas de densificación por flujo viscoso daban lugar a mullitas sinterizadas con densidad cercana a la teórica y fina micro-estructura. Altas velocidades de densificación (o,5% a 1%/min) son las mas adecuadas para sinterizar mullita de alta densidad. Flujo viscoso de la sílice amorfa es el mecanismo que controla la velocidad del proceso antes de disolver la alúmina y formar mullita por un proceso de nucleación y crecimiento. Se observan también desviaciones del modelo lineal de Frenkel para el flujo viscoso.

Palabras clave: mullita, coloidal, sol-gel, cinética, dilatometría.

1. INTRODUCTION

Mullite (3Al2O3·2SiO2) is well-known as a superior engineering ceramic material. Dense high purity mullite with fine grains offers excellent properties such as low theoretical density, low thermal conductivity, low thermal expansion, low dielectric constant and excellent high temperature strength, thermal shock resistance, chemical stability, low creep rate and good transmission in the mid-infrared band (1). Advanced ceramics based on mullite are excellent candidates for advanced ceramic applications for structural, electronic and optical applications such as engine components, thermal insulation parts, gas filters,substrates in fast electronic devices, heat exchangers, multilayer packaging, and window material in the mid-infrared range. It is also used in ceramic fibres and matrices of ceramic matrix composites. Mullite is also a key material required for ceramic matrix composites for environmental barrier coatings (1-3) More recently a renewed interest on mullite based materials has appeared in the literature due to new materials requirements in emerging technologies. Pyzik et al (4) had developed Diesel particulate filters produced from acicular mullite. These filters have demonstrated high filtration efficiency, low-pressure drop, fast regeneration, high temperature chemical resistance, and high mechanical integrity. The ability to control microstructure, porosity, and pore size distribution allows

these materials to be tailored to meet the requirements of deep bed filtration and fine particulate emission control. This high add value component for car industry based on mullite is a clear evidence of the now a days interest on mullite-based materials such as mullite-refractory metals composites for high/low temperature components, thermal barrier coatings, electrical conductor/insulator components (HID2 and cool LED3 lamps), as well as for multifunctional devices (1,3)

Mullite is the only binary compound in the SiO_2–Al_2O_3 system. It is a solid solution with stable composition which displays various Al to Si ratios referring to the solid solution $Al_{4+2x}Si_{2-2x}O_{10-x}$, with x ranging between about 0.2 and 0.9 (about 55 to 90 mol% Al_2O_3). The end members of these ranges have compositions $2Al_2O_3.SiO_2$ and $3Al_2O_3.2SiO_2$ (referred to as 2:1 and 3:2 mullite, respectively). These types of mullite, when developed in multi-component materials, such as porcelain bodies produced from kaolin–alumina mixtures, are named primary and secondary mullite (5).

Mullite has been prepared by different techniques and from a variety of starting materials all of which follow more or less different mullitization routes on heating. The main reason for the different mullitization routes is attributed to the different degree of mixing of the Al_2O_3 and SiO_2 in the grains and on a molecular scale, respectively

There exists general agreement that the scale of chemical homogeneity of the precursors plays an important role in the mechanisms of mullite formation and thus determines the temperature range were total mullitization is achieved. Precursors obtained by colloidal or polymeric techniques show considerable differences in short range atomic arrangement and very dissimilar thermal behaviour Mullite formation above 1200 ºC via γ-Al_2O_3 precursor is observed in mixtures of kaolinite and alumina, sol mixtures and diphasic (colloidal) gels while direct formation of Al-rich mullite at about 900–1000 ºC is observed in monophasic (polymeric) gels and glasses. Single-phase precursors exhibit direct mullitization from the amorphous state at temperatures as low as 950 ºC, while diphasic precursors mullitize above 1200 ºC by the reaction of transient spinel type alumina with silica (6-7). The specific temperature of mullite formation from monophasic gels depends on several experimental parameters, such as the conditions for hydrolysis of alkoxide reagents for obtaining the gel precursors and the rate of heating gel precursors. The advantages provided by these methods are good mixing, chemical homogeneity, high purity, stoichiometric compounds, selected range of compositions and faster reaction time than solid state processes. Little work has been reported on the controlling step of mullitization from monophasic gels. The major rate controlling steps for nucleation and nucleation-growth were thought to be nucleation controlled (8-9) and diffusion of Si ions in the amorphous matrix.

Several research groups investigated the kinetics and mechanisms of mullite crystallization from diphasic precursors of various natures (10-15). The variation in the activation energy of mullite formation found by many authors could be partly due to different crystallization processes and partly due to differences in the experimental conditions used in the determination of the activation energy. There is in any case an agreement that the formation and growth of mullite from diphasic alumino-silicate gels occurs via a nucleation and growth mechanism. In order to reduce the activation energies of diphasic mullite precursors, doping of the starting compounds has been proposed (for instance using P_2O_5, B_2O_3, or TiO_2) because it reduces the viscosity of the amorphous silica, increasing the diffusion rates and thus accelerating the nucleation and crystal growth of mullite (16). There are, however, different opinions on the rate controlling step of this process. Wei and Halloran (10) investigated the mullitization kinetics of diphasic gels and proposed a mechanism involving either interface-control or control by short-range diffusion near the interface. Subsequent growth of mullite is controlled by the dissolution of alumina in the siliceous matrix not by interdiffusion through mullite. They suggest that the mullitization process occurs via nucleation and crystallization of mullite crystals within the matrix as the matrix reaches the saturation concentration necessary to provide mullite nucleation. Li and Thomson (11) observed a Y-Al_2O_3 first crystalline phase. Hulling and Messing (12) considered that release of alumina from the initially-formed Y-Al_2O_3 structure is the rate-controlling step in mullitization from diphasic and hybrid gels. Sundaresan and Aksay (13) reported a similar rate limiting mechanism for the growth of mullite nuclei in the mullitization of a diphasic gel and also suggested that mullitization is no limited only by alumina dissolution (release) at low temperatures (<1350 ºC), but by diffusion at high temperatures (<1650 ºC). Based on this model, the Ea for diffusion in the amorphous aluminosilicate matrix must be smaller than that of alumina released from the Y-Al_2O_3 structure in type (1) starting materials. A summary of the Ea values found from various starting materials and a discussion of the reasons for the unusually large Ea values for mullitization has been recently published (6).

On the other hand, Brinker and Scherer (18) have also reported that mullite sintering of Al203-SiO2 colloids is controlled by the competition between mullite crystallization via viscous flow and densification; full density processing involves increasing the heating rate to delay crystallization. This mechanistic interpretation of the competition between viscous flow densification and mullite crystallization has been reported by many authors (10). A book entitled "Mullite" (19), and special issues of the JACS (20) and the JECS (21) contain numerous other references to the same topic. It is also reported that the problem of viscous densification deceleration by crystallisation is different from solid state systems in geometry, transport mechanisms, etc, where grain growth control can result in better densification.

In this context, the present work, is focused on investigating both the sintering and crystalization kinetics of silica-alumina diphasic mullite gels using non- isothermal conditions involved in the constant heating rate (CHR) and rate control sintering dilatometer experiments. This technique has been used by Brinker et al (17) and Orgaz (26) to study the densification kinetics of homogeneous porous silica gels and the different operating mechanics that occur during this sintering process. The changes of the maximum values of the shrinkage rate with temperature can be interpreted similarly to the shifting of the crystallization rate curves with heating rate using DTA and DSC experiments. Our interest is to analyse the potential of dilatometer experimental curves to obtain information about the sintering and crystalization process, the mechanisms involved, and the rate controlled steps. This analysis is carried out by comparing the predictions of the CHR equations with the results obtained by other researchers using different analysis techniques. Also the objective of this paper to know what is the response of the diphasic mullite samples to different programmed constant densification rates

and to determine the optimal temperature time profile to obtain a fine full density grained mullite.

2. EXPERIMENTAL PROCEDURE

Gels of the stoichiometric mullite composition (3 Al_2O_3- 2 SiO_2) were prepared by mixing colloidal alumina and silica sols at pH below 3. The starting precursors were a colloidal fumed silica (cab-O-Sil EH-5) with a specific surface area of 390 m2/g and a particle size of 7 nm and a colloidal aluminium oxide C from Degussa with similar characteristics. The sol was obtained by gradual and sequential addition of first silica and then alumina into acid water contained in a high shear blender. The suspension was always kept at pH below 3 and finally maintained for half an hour, after which a few drops of HF were added to considerably reduce the gelling time. The resulting gels had a BET surface area of 110 m2/g. The gels were crushed and sieved below ‹25 microns. Rods of isostatic pressed powders (2500 Kg/cm2), formed for dilatometry experiments,had a green density of 45% of the theoretical density. CHR and RCS non- isothermal experiments were performed using a Linseis dilatometer which allowed continuous monitoring of the axial shrinkages of the samples at heating rates of 2, 10 and 20 K/min up to 1650ºC after which the samples were cooled rapidly. The dilatometer was also equipped with suitable software to carry out the corresponding RCS tests in the range 0,1 to 2% densification per minute. The microstructure of selected samples was observed by Scanning Electron Microscopy of fractured samples. A diffractometer (Siemens D500) equipped with high temperature camara was employed to continuously register phase changes with temperature.

3. THEORETICAL APPROACH

3.1.-Isothermal and non isothermal crystallisation kinetics.

Most of the kinetics studies of mullitizacion have been analysed and determined by various methods using both powders and bulk samples and under either isothermal or non isothermal conditions. Techniques such as DTA, DSC and X-ray diffraction are widely used (6).

The theoretical basis for interpreting crystallisation results under isothermal conditions is provided by the Johnson-Mehl- Avrami (JMA) solid state transformation theory, which describes the evolution of the crystallisation fraction, x, with the time, t, during a phase transformation under an isothermal condition

$$1\text{-}x = \exp(-(kt)^m) \quad [1]$$

Where x is the volume fraction crystallised after time t, m is the Avrami exponent and k is the rate of nucleation growth (k) whose temperature dependence is generally expressed by the Arrhenian-type equation.

$$K = k_0 \exp(-(Ea^{NG}/RT)) \quad [2]$$

where k0 is the frequency factor, Ea is the apparent activation energy for nucleation-growth (Ea^{NG}) and R is the ideal gas constant.

Under non-isothermal conditions, using DTA or DSC curves, the Ea has been calculated from the variation of the peak temperature measurements against the heating rates. Many mathematical equations have been proposed for the calculation of the activation energies, although the Kissinger equation (Eq. (4)) is most commonly used (22).

$$\mathrm{Ln}(T_p^{\,2}/\phi) = \ln(Ea/R) - \ln \nu + Ea/(RT_p) \quad [3]$$

Or

$$\mathrm{Ln}(\phi/T_p^{\,2}) = -Ea/(RT_p) + C \quad [4]$$

where T_p is the temperature of the exothermic peak top (crystallization temperature), ϕ the heating rate and ν is the frequency factor, Ea is the activation energy for nucleation and growth, R is the universal gas constant and C is a constant.

Another kinetic approach derived by Marseglia (23) from the Avrami solid-state transformation fenomenological expression results in a linear relationship between Ln (ϕ/Tp) versus 1/Tp where Tp is the temperature at which the maximum peak appears. A plot of Ln (ϕ/Tp) against 1/Tp yields a straight line from which a value of Ea can be derived if a value of m is assumed.

According to Augis and Bennet (24), the crystallization mechanisms can be determined from the Avrami exponent, m, of the exothermic peak represented by:

$$m = 2{,}5\, Tp^{\,2} R / \Delta T\, Ea \quad [5]$$

where ΔT is full width at half maximum of the exothermic peak (FWHM). Knowing the activation energy from the Kissinger plot, the Avrami exponent can be calculated.

Values of m for various crystallisation mechanisms have been obtained by Matusita et al (25)

1.2 Shrinkage constant heating rate analysis

The Avrami expression has also been used to describe the kinetics of isothermal viscous sintering of glass powders. According to this phenomenological equation, the fraction $\Delta L/Lo$ of material densified after a time t is given by

$$Z = \Delta L/Lo = 1 - \exp(-At^{\,m}) \quad [6]$$

Where m is a constant dependent on the details of densification mechanisms, A is related to the rates of the sintering and Z the completed fraction of the total shrinkage.

In the non-isothermal CHR method, the specimen temperature is increased at a constant rate ($dT/dt = \phi$) and the shrinkage rate is determined as a function of temperature. The most widely theoretically derived equations used to

analyse for CHR experiments data are described as (27):

$$Z^{n+1} = K_0 RT^2 (n+1) \,/\, \phi\, Q.\exp(-Q/RT) \quad [7]$$

$$T^2 (dZ/dt) \,/\, \phi = (Q/(n+1)R).Z \quad [8]$$

where Z is the linear shrinkage ΔL/Lo, and Q the activation energy and n, a geometric factor, are characteristics of the rate controlling mechanism. For viscous sintering n=0 and K0 = constant.Thus, under CHR conditions, a plot of Ln Z versus 1/T gives a straight line with a slope very near – Q/(n+1)R and a plot T^2 (dZ/dt)/ ϕ versus Z gives a straight line with slope Q/(n+1)R. From eq.6 a plot of ln(ΔL/Lo) versus Ln (heating rate) at constant temperature results in a straight line of slope – 1/(n+1). Substitution into –Q/(n+1)/R then gives Q.

Equations 6 and 7 are based on the assumption supported by experimental results that

$$(dz/dt)\ \text{isotherm} = (dz/dt)\ \text{non isotherm}$$

for the general equation given for isothermal initial- staqe sintering

$$dZ/d.t = Z^{-n} Ko.\exp(-Q/RT) \quad [9]$$

This rate law equation through which the sintering process mechanism can be identified is usually applied for CHR conditions. At constant temperature, the isothermal kinetics predicted can be then expressed as

$$z = K.\, t^{1/n+1} \quad [10]$$

where n is the CHR sintering kinetics parameter. For n=0, Z= ΔL/Lo is proportional to time which coincides with the Frenkel model to describe sintering at the initial-stage.

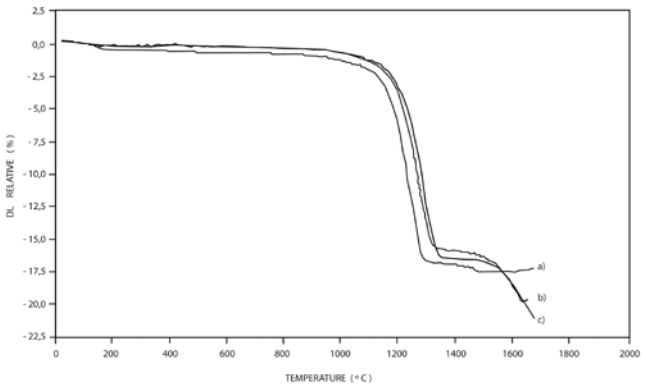

Fig. 1- Relative shrinkage against temperature for different heating rates: a) 2 K/min b) 10 K/min and c) 20 K/min.

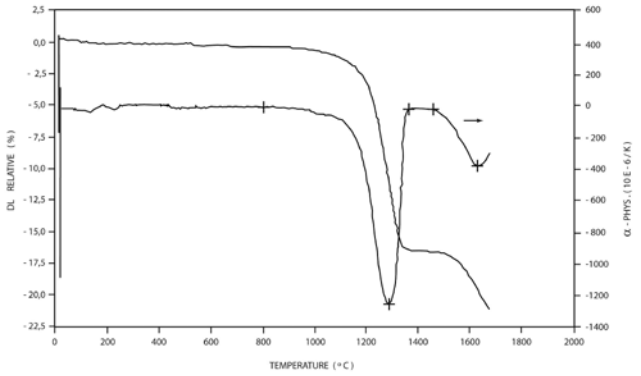

Fig. 2- Effect of heating rate on the temperature at maximum shrinkage rate in CHR dilatometer experiments. a) low temperature peak b) high temperature peak.

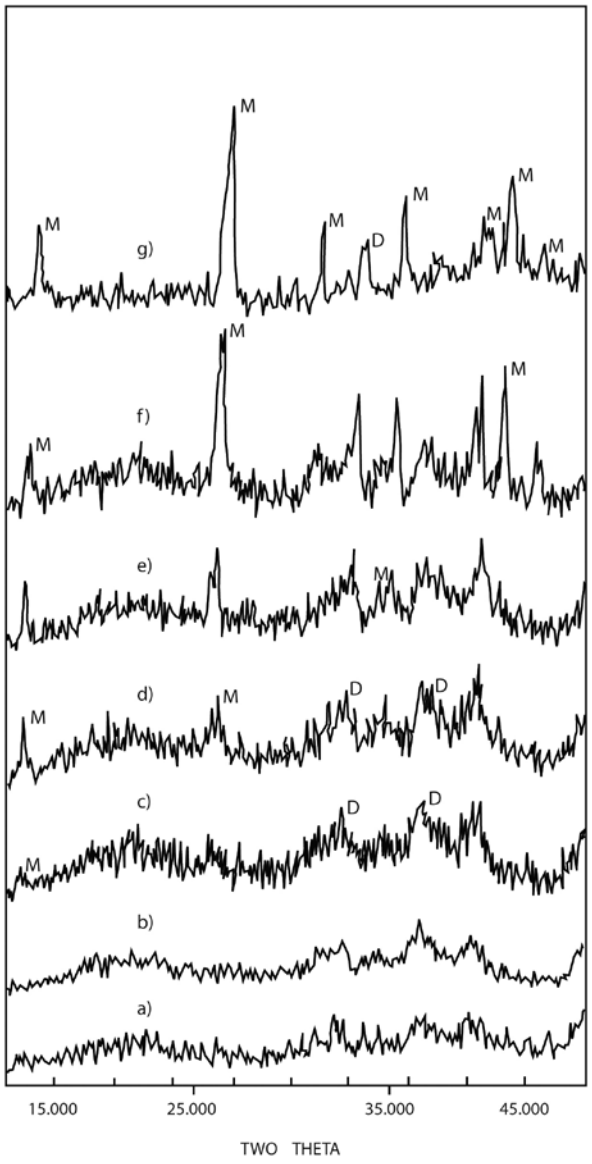

Fig. 3- High temperature X-ray diffraction of mullite diphasic gels.
a) 1100 ºC; b) 1200 ºC; c) 1275 ºC; d) 1300 ºC; e) 1310 ºC; f) 1325 ºC; g) 14000 ºC.
M: mullite; D: Delta alumina.

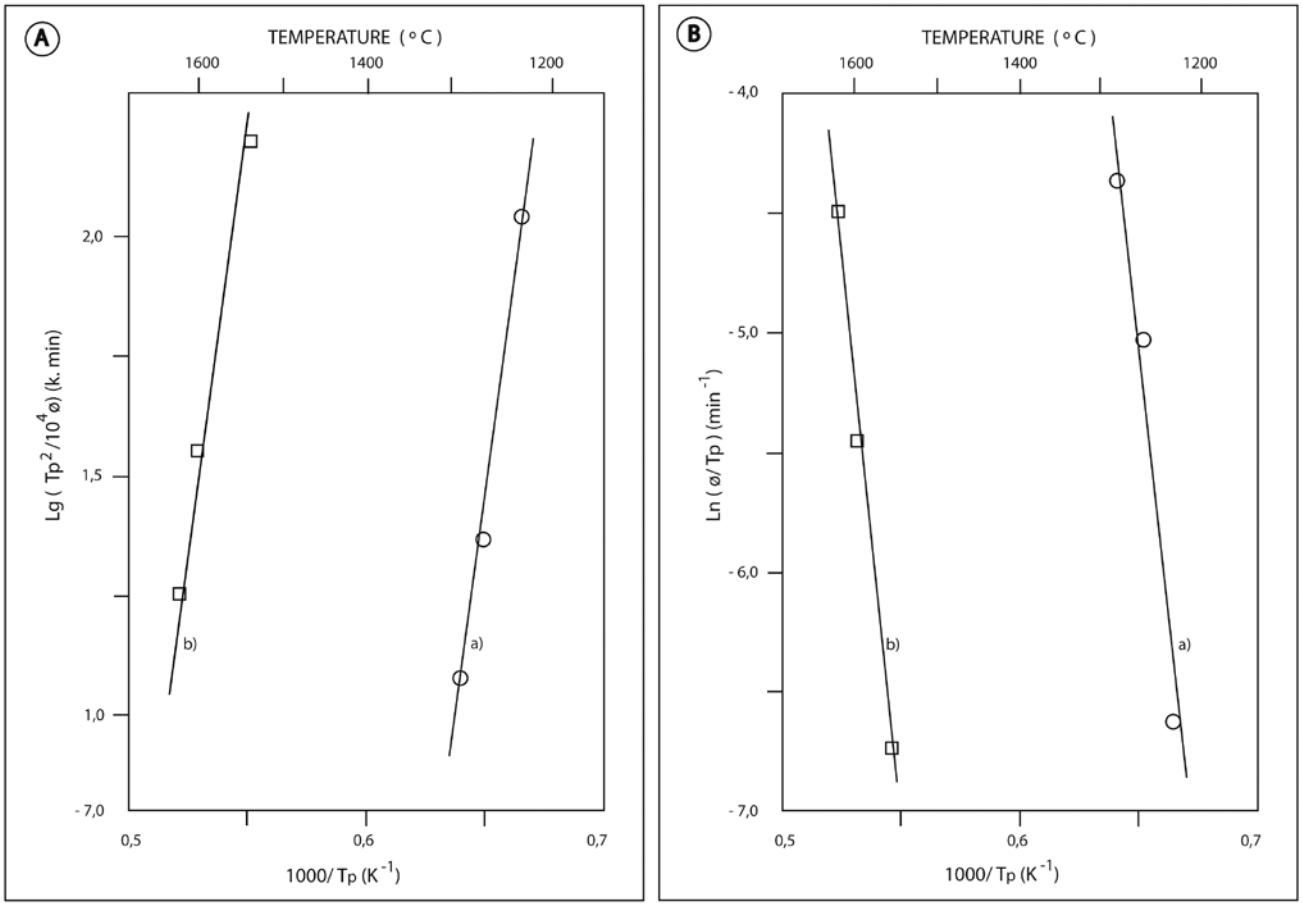

Fig. 4- Plots according to Kissinger and Marseglia equations.

4. EXPERIMENTAL RESULTS AND DISCUSSION

4.1.- Effect of constant heating rate on the mullite crystallization process.

Figure 1 shows values for the relative linear shrinkage ΔL/Lo versus temperature, T, at three different heating rates. The curves show similar shape and are generally shifted to higher temperatures with increasing heating rate. At temperatures ‹13OO ºC the slower the heating rates, the higher the linear shrinkage at any temperature. However at temperatures above 13OOºC a nearly plateau ranging from approximately 1300 to 1500ºC was found for all samples from which shrinkage was produced again. Higher shrinkage values were observed for samples which were fired at the higher heating rate of 20 K/min. For the samples sintered at the lowest heating rate of 2 K/min, no shrinkage was observed after the plateau was formed.

By measuring the tangent of the curves at a given temperature and by utilizing the equation dT = ϕ dt, the shrinkage rate, d ΔL/Lo /dt, was determined for a particular temperature. It was observed that the shrinkage rate varied with temperature to reach a maximum value and then decreases. Two maxima were found (Figure 2). The temperature at which the first maximum value occurs depends on the heating rate used and changes between 1230 and 1290 ºC. The maximum of the curves shifts to higher temperatures with increasing heating rate. A second maximum shrinkage rate value was also found at temperatures above 1500 ºC which also moves to higher temperatures with increasing heating rate. For the heating rates of 2 K/min small variations in the shrinkage rate causing the high temperature peak were found due to the low densification produced in this interval of temperatures. However significant changes in the shrinkage rate of the high temperature peak were found for the higher heating rates. Figure 3 shows high temperature X-ray diffraction results of the gels confirming that mullite crystallization is observed at temperatures around 1275 ºC and changes from gamma to alfa alumina are observed.

A comparison between the Kissinger and Marseglia equations (Figures 4A and 4B) yield a straight line for each of the two peaks found for each heating rate in the whole range of temperature up to 1650 ºC and values of m close to 1. Both straight lines are nearly parallel and can be associated to the nucleation and crystal growth mechanisms respectively. Values close to 1 have been interpreted in porcelain stoneware as a bulk nucleation dominant mechanism in mullite crystallization followed by three dimensional growth of mullite crystals with polyhedron-like morphology controlled by diffusion from a constant number of nuclei (28). Values of m=1 for viscous sintering can be inferred from the Avrami-type equation derived by Kingery et al (29) from the Mackenzie-Shuttleworth viscous sintering model and verified by Gres et al (30). Values of m=1 for a mechanism of interface reaction for bulk (constant number of nuclei) and surface nucleation in one-dimensional crystals were referred by Matusita et al (25).

The obtained activation energy of 778 KJ/mol is below the values of 1070 (200) found by Wei and Halloran (10) below the

values of 935 (14) and 1119 (25) found by Tkalcec (14) and below the values of 1034 (37) and 1108 (44) found by Li and Thomson (11) for diphasic gels. This can be explained by a higher amount of glass phase and a lower viscosity of the mullite gels studied in this paper as a consequence of a better homogenization and a higher water content or other experimental conditions, such as particle size, particle distribution, packing state, etc.. The activation energy obtained is close to those obtained by Lee and Yu (31) for co-precipitated gels and by Hulling and Messing (12) for hybrid gels and higher than those values obtained for porcelain stoneware 622 kJ/mol (28)

4.2. Effect of the constant heating rate on the shrinkage process.

Figure 5 show plots as expressed by equation 7. Several different slopes appear. A change in slope implies that n and/or Q change, i.e, that there is an apparent change in the predominant shrinkage controlling mechanisms. The experimental- results can be represented by several straight lines or regions. A first low slope straight line (Region I) up to 1070 to 1100 ºC and 0.7 to I.5 % shrinkage is observed which can be associated to condensation- polymerization because shrinkage in this region is accompanied concurrently by loss of water. After a gradual transition a second higher slope straight line (Region II) appears at temperatures of approximately 1050 up to 1265 to 1290 according to the heating rate used. Such straight lines are parallel and therefore a similar sintering mechanism seems to be involved. As seen before, viscous flow sintering is the rate-controlling mechanism for this densification region. Relative shrinkages of 15 to 17% and relative densities of 0.72-0.76 are reached. A third nearly horizontal very low slope straight line (Region III) was found between 1265-1290 to 1510 ºC, approximately, where low densification exists. This behaviour can be related to high crystal growth of mullite which prevents (2 K/min heating rate) or shifts to higher temperatures the densification process (20 K/min heating rate) (Region IV). As seen at low heating rates of 2K/min no further densification is obtained at temperatures above 1300ºC, which is caused by the large grain size of the mullite crystals which prevent higher densification. At heating rates of 20 K/min the material densifies at higher temperatures after mullitization. This competition between densification and crystal growth is well known (18).

Data obtained from the linear region II of Figure 5 are plotted in Figure 6 as Log of shrinkage against Log heating rate for several temperatures comprised between 1050 and 1300 ºC. Straight lines are formed from which n values were calculated from the slope = -1/(n+1). Figure 7 displays the n changes with temperature. As observed for the range of temperature where viscous flow densification occurs, the n values change from n=0 obtained at 1050 ºC to n=2.2 values obtained up to 1200 ºC. At higher temperatures the n parameter increases considerably. Values of n=2.2 for viscous flow are apparently in contradiction with values of n=0 established by the initial-

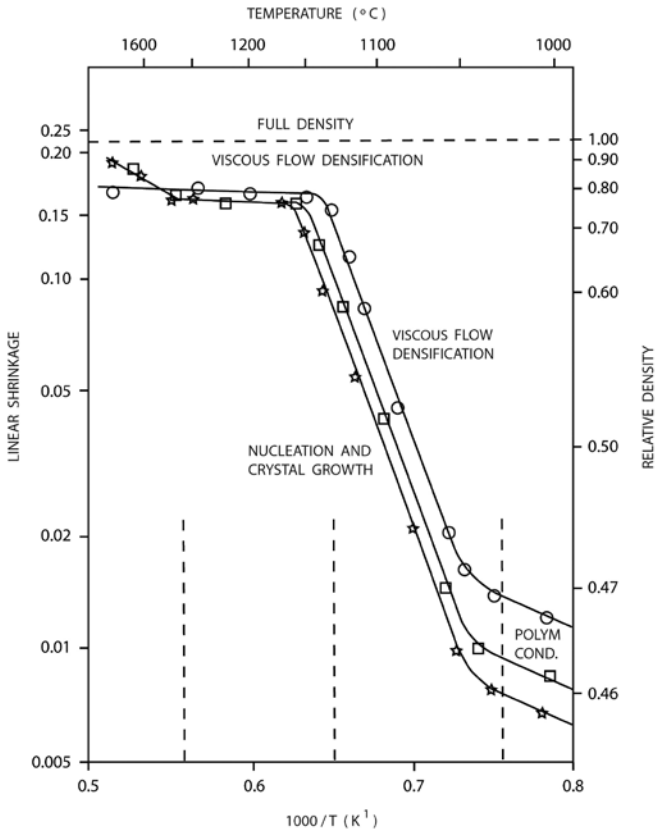

Fig. 5- Ln shrinkage as a function of 1/T (K^{-1}) plots for CHR experiments at various heating rates of a) 2 K/min b) 10 K/min and c) 20 K/min.

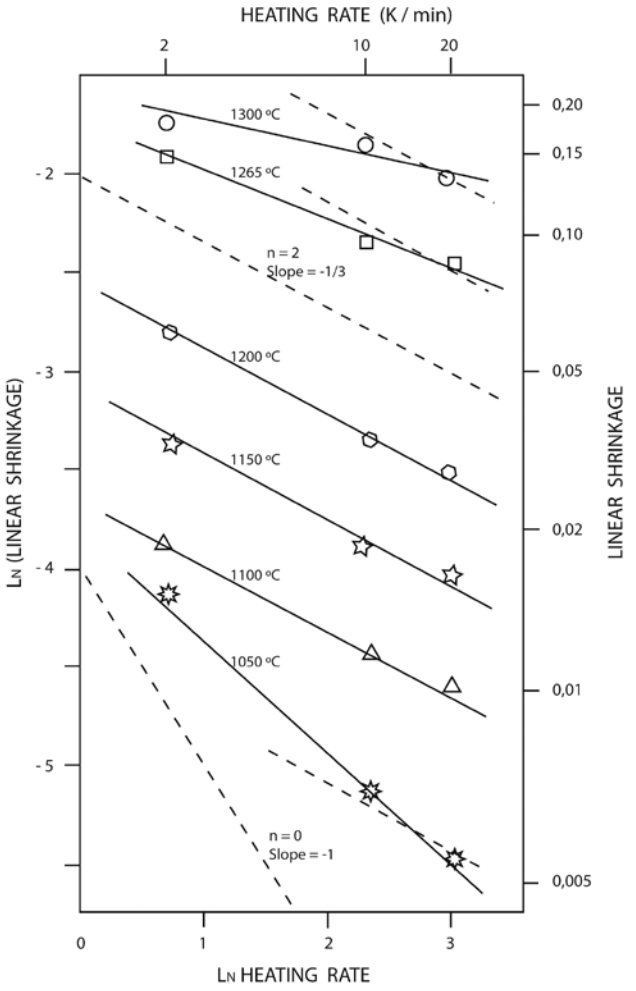

Fig. 6- Ln heating rate against Ln linear shrinkage between 1050ºC and 1300 ºC.

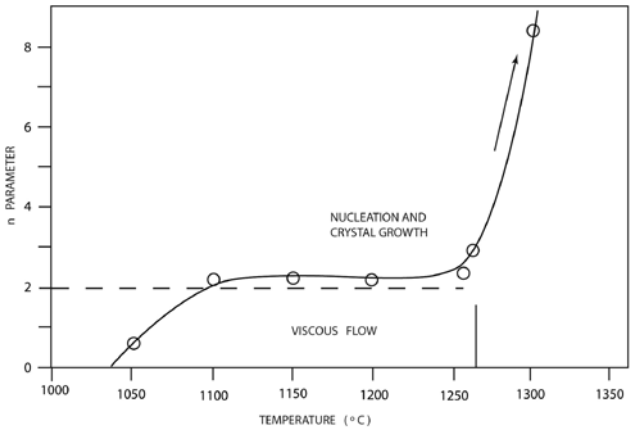

Fig. 7- Constant heating rate sintering parameters n as a function of temperature.

stage neck-growth Frenkel model for ideally viscous flow sintering at the early stage (32). This model predicts a linear relationship between linear shrinkage and time given by the equation:

$$Z = 3\,\gamma\,t/8\,\eta\,a \qquad [11]$$

where z is the linear shrinkage, t is the isothermal sintering time, a is the glass sphere diameter, η viscosity and γ the surface tension. Values of n=2.2 or higher indicate a deviation of ideal viscous flow Frenkel model due to nucleation and crystallization of mullite crystals. Very high n values at temperatures above 1260 ºC are the result of the effects of crystalline growth on shrinkage. Large n values are explained by the competition between crystallization and densification, producing lower densification than that produced by the viscous flow Frenkel model to describe sintering at initial-stage. These results confirm the assumption suggested by Sundaresan and Aksay (13) that diphasic gel sintering of mullite is rate controlled by viscous flow of the amorphous silica till nucleation and crystal growth of mullite occurs via alumina dissolution.

4.3. Constant densification rate sintering results

Constant densification rate experiments allow theoretical density-time profiles to be scheduled and the experimental deviation for each program to be analysed. They also the most suitable kinetics leading to nearly full density to be established.

Figure 8 displays changes of relative shrinkage with temperature for samples which were scheduled to have a constant densification rate of 0,5% linear per minute.

Different total shrinkages, final densities and microstructural developments were found for firing schedules of 0,1%/min and 1%/min. For low densification rates (0.1 %/mín) deviations between experimental and scheduled density-time profiles were produced. The samples could not follow the full density-time profile as scheduled and therefore low final densities were found. Large grain growth and a remaining porosity were also observed. For samples densified following a controlled intermediate (0,5 %/min) or a high densification rate (l%/min) program a nearly full-density was attained with uniform and very fine final microstructure (Figure 9). No deviations between experimental and scheduled time-density profiles were noticeable.

These rate-controlled experiments confirm that in the temperature zone where crystallization kinetics are relevant fast firing processes must be profiled. These results indicate that rate controlled sintering at intermediate (0,5% per minute) or at high densification rates (1% /mín) are more suitable than those performed at low densification rates to sintering full density mullite.

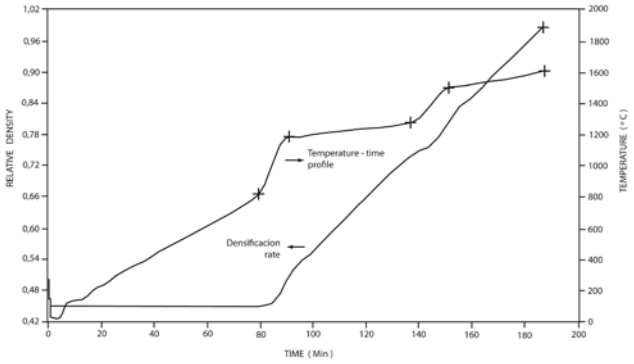

Fig. 8- Rate controlled sintering. 0,5% /min density-time schedule and the corresponding temperature-time profile.

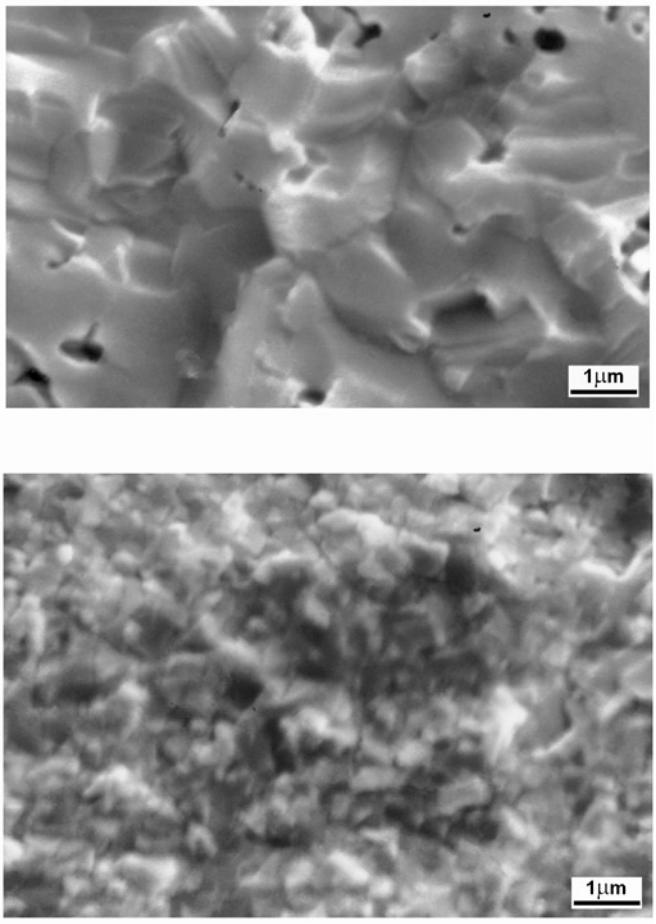

Fig. 9- Scanning electron microscopy of mullite sintered at different scheduled densification rates. A) 0,1%/min b) 1%/min.

5. CONCLUSIONS

The results of this study indicate that CHR and RCS dilatometry are suitable techniques to study the complex processes of sintering and crystallization operating during the transformation of gel to dense mullite. The results of CHR sintering dilatometer experiments performed on colloidally processed sol-gel mullite show that both the Arrhenius and the shrinkage rate plots are useful to describe the sintering mechanisms involved because they permit the identification of slope changes. Condensation-polymerization, viscous flow, mullitization and final viscous flow densification are the operating processes. Densification starts at approximatelly 800 ºC by a condensation reaction which eliminates residual OH groups. The densification process is mainly rate-controlled by viscous flow of the amorphous silica till nucleation and crystallization of mullite appears via alumina dissolution. Mullitization onsets at approximately 1230 ºC which shifts to higher temperatures with increasing heating rates. Mullitization slows down or prevents further densification.

REFERENCES

1. R.Torrecillas, J.M. Calderon and J.S.Moya. J.Eur.Ceram.Soc. Suitability of mullite for high temperature applications. J. Eur. Ceram.Soc. 19,13-14, 2519-2527 (1999).
2. S.Somilla and Y. Hirata. Mullite powder technology and applications in Japan. Am.Ceram.Soc. Bull. 70,10, 1624-32 (1991).
3. I.A.Aksay, D.M.Dabbs and M.Sarikaya. Mullite for structural, electronic and optical applications J.Am.Ceram.Soc 74,10, 2343-2358 (1991).
4. A.J. Pyzik. New design of a ceramic filter for diesel emission control applications. Int.J.Appl.Ceram.Technol. 2,6,440-451 (2005).
5. H.S.Schneider, J.Schreurer and B.Hildmann. Structure and properties of mullite. A review J.Eur.Ceram.Soc. 28,2,329-344, (2008).
6. K.Okada. Activation Energy of mullitization from various starting materials. J.Eur.Ceram.Soc, 28,2, 377-382, (2008).
7. F.Griggio, E.Bernardo, P.Colombo and G.L.Messing. Kinetic studies of mullite synthesis from alumina nanoparticles and a ceramic polymer. J.Am. Ceram.Soc. 91, 8, 2529-2533, (2008).
8. D.X Li and W.J. Thomson. Mullite formation kinetics of a single phase. J.Am.Ceram.Soc 73,4,964-969, 1990.
9. T.Takei, Y. Kameshima, Y.Yasumori and K.Okada.Crystallization kinetics of mullite in alumina-silica glass fibers. J.Am.Ceram.Soc 82,10, 2876-2880, (1999).
10. W.Ch Wei and J.W.Halloran. Transformation kinetics of diphasic aluninosilicate gels J.Am.Ceram.Soc. 71,7,581-587, (1988).
11. D.X. Li and W.J. Thomson. Mullite formation from nonstoichiometric diphasic precursors. J.Am.Ceram.Soc.74,10, 2382-2387, (1991).
12. J.C.Hulling and G.L.Messing. Epitactic nucleation of spinel in aluminosilicate gels and its effect on mullite crystallization. J.Am.Ceram.Soc. 74,10, 2374-2381, (1991).
13. S.Sundaresan and I.A.Aksay. Mullitization of diphasic aluminosilicate gels. J.Am.Ceram.Soc 74,10, 2388-2392 (1991).
14. E.Tkalcec, H.Ivankovic, R.Nass and H.Schmidt. Crystallization kinetics of mullite formation in diphasic gels containing different alumina components J.Eur.Cera.Soc. 23,9,1465-1475, (2003).
15. E.Tkalcec, S.Kurajica and H.Ivankovic. Diphasic aluminosilicate gels with two stage mullitization in the temperature range of 1200-1300ºC J.Eur.Cera. Soc. 25,5,613-626, (2005).
16. S.H.Hong and G.L.Messing. Mullite transformation kinetics in P_2O_5- TiO_2- and B_2O_3- doped aluminosilicate gels. J. Am. Ceram. Soc, 80,6, 1551-1559 (1997).
27. C.J.Brinker, W.d.Drotning and G.W.Scherer. Better ceramics through chemistry 1984.
18. C.J. Brinker and G.W. Scherer. Sol-gel Science. The physics and chemistry of sol gel processing. Elsevier Science and Technology.1990.
19. Mullite. (Ed) H.Schneider and S.Komarneni. Wiley.Inter Science. 2005.
20. International Workshop Mullite 2006.Hartmut Schneider. J. Eur.Ceram. Soc. 28, 2, (2008).
21. Symposium of mullite processing, structure and properties. J.Amer.Ceram. Soc.74,10 (1991).
22. H.E. Kissinger. Reaction kinetics in Differential Thermal Analysis. Analytical. Chemistry. 29,11, 1702-1706 (1957).
23. E. Marseglia. Kinetic theory of crystallization of amorphous materials. J.Non-Cryst Solids 41,1,31-36 (1980).
24. J.A.Augis and J.B.Bennet. Calculation of the Avrami parameters for heterogeneous solid state reactions using a modification of the Kissinger method. J. Therm.Anal. 13, 2, 283-292, (1978).
25. K.Matusita, K.Miura and T.Komatsu. Kinetics of non isothermal crystallization of some fluorozirconate glasses Thermochim.Acta. 123,15,263-270 (1985).
26. F.Orgaz-Orgaz. Densification kinetics of porous colloidal P_2O_5 doped silica gels. J.Non Cryst Solids 100,1-3, 263-268, 1988.
27. J.L.Woolfrey and M.J.Bannister. Non isothermal techniques for studying initial stage sintering. J.Am.Ceram.Soc. 55,8, 390-394, (1972).
28. M.Romero, J.Martin and J.Rincon. Kinetic of mullite formation from porcelain stoneware body for tiles production. J.Eur.Ceram.Soc 26,9, 1647-1652, (2006).
29. W.Kingery, H.Bowen and D.Uhlman. Introduction to Ceramics. Wiley.New York,1976.
30. E.Greiss, C.Cuerci, C.Walker and S.Wen. Isothermal sintering of spheroidized cordierite-type glass powders. J.Amer.Ceram.Soc. 68,12, C-328-C-329 (1985).
31. J.S.Lee and S.C.Yu. Mullite formation kinetics of coprecipitate Al2O3-SiO2 gels. Mat. Research Bull. 27,4, 405-416 (1992).
32. J.Frenkel. J. Phys (Moscow), 9, 385 (1945).

Recibido: 10.07.08
Aceptado: 05.12.08